NREL
NATIONAL RENEWABLE ENERGY LABORATORY

Short-Circuit Modeling of a Wind Power Plant

Preprint

E. Muljadi and V. Gevorgian

To be presented at the Power & Energy Society General Meeting
Detroit, Michigan
July 24-29, 2011

NREL is a national laboratory of the U.S. Department of Energy, Office of Energy Efficiency & Renewable Energy, operated by the Alliance for Sustainable Energy, LLC.

Conference Paper
NREL/CP-5500-50632
March 2011

Contract No. DE-AC36-08GO28308

Available electronically at http://www.osti.gov/bridge

Available for a processing fee to U.S. Department of Energy
and its contractors, in paper, from:

U.S. Department of Energy
Office of Scientific and Technical Information

P.O. Box 62
Oak Ridge, TN 37831-0062
phone: 865.576.8401
fax: 865.576.5728
email: mailto:reports@adonis.osti.gov

Available for sale to the public, in paper, from:

U.S. Department of Commerce
National Technical Information Service
5285 Port Royal Road
Springfield, VA 22161
phone: 800.553.6847
fax: 703.605.6900
email: orders@ntis.fedworld.gov
online ordering: http://www.ntis.gov/help/ordermethods.aspx

Cover Photos: (left to right) PIX 16416, PIX 17423, PIX 16560, PIX 17613, PIX 17436, PIX 17721

Printed on paper containing at least 50% wastepaper, including 10% post consumer waste.

Short-Circuit Modeling of a Wind Power Plant

E. Muljadi
Fellow, IEEE
eduard.muljadi@nrel.gov

V. Gevorgian
Member, IEEE
vahan.gevorgian@nrel.gov

National Renewable Energy Laboratory
1617 Cole Blvd.
Golden, CO 80401, USA

Abstract - An important aspect of wind power plant (WPP) impact studies is to evaluate short-circuit current (SCC) contribution of the plant into the transmission network under different fault conditions. This information is needed to size the circuit breakers, to establish the proper system protection, and to choose the transient suppressor in the circuits within the WPP. This task can be challenging to protection engineers due to the topology differences between different types of wind turbine generators (WTGs) and the conventional generating units.

This paper investigates the short-circuit behavior of a WPP for different types of wind turbines. The short-circuit behavior will be presented. Both the simplified models and detailed models are used in the simulations and both symmetrical faults and unsymmetrical faults are discussed.

***Index Terms* — Fault contribution, induction generator, protection, short circuit, wind power plant, wind turbine.**

I. Introduction

Energy and environmental issues have become one of the biggest challenges facing the world. In response to energy needs and environmental concerns, renewable energy technologies are considered the future technologies of choice [1], [2]. Renewable energy is harvested from nature, and it is clean and free. However, it is widely accepted that renewable energy is not a panacea that comes without challenges. With the federal government's aggressive goal of achieving 20% wind energy penetration by 2030, it is necessary to understand the challenges that must be overcome when using renewable energy.

In the years to come, there will be more and more wind power plants (WPPs) connected to the grid. With the goal of 20% wind penetration by 2030, the WPP's operation should be well planned. The power system switchgear and power system protection for WPPs should be carefully designed to be compatible with the operation of conventional synchronous generators connected to the same grid. This paper attempts to illustrate the behavior of short-circuit current (SCC) contributions for different types of WTGs.

Conventional Power Plant versus Wind Power Plant

A conventional power plant consists of a single or several large (e.g., 100 MW) generators. The prime mover of the generator can be steam, gas, or a combustion engine. The generator is controllable and is adjustable up to a maximum limit and down to minimum limit. The power output is dispatched according to the load forecast, influenced by human operation, and is based on optimum operation (i.e., scheduled operation). The power plant is usually located relatively close to the load center.

The typical, conventional generator used is a synchronous generator. The rotational speed is fixed – no slip; and the flux is controlled via exciter windings. The magnetic flux and the rotor rotate synchronously.

A WPP consists of many (hundreds) of wind turbine generators (WTGs). Currently, available WTG sizes are between 1 MW and 5 MW. The prime mover of the WTG is wind, and it is free, natural, and pollution-free. The controllability of the WPP is typically curtailment (spilling the wind). The energy production of a WPP depends on the wind variability, and its dispatch capability is based on wind forecasting, and it is influenced more by nature (wind) than human factors, with the goal set on maximizing energy production from renewable resources (i.e., unscheduled operation). Large-scale WPPs are located in a high-wind resource region, and these may be far from the load center.

Because a WPP covers a very large area, there are power output diversities found in a typical WPP. Each WTG in a WPP will be located at different electrical distances from the substation (diversity in line impedance). Each turbine may be driven by different instantaneous wind speeds. Thus, the operating condition of each turbine may be slightly different from others within the WPP.

Operation of Wind Turbine Generator

The generator at each turbine should be protected individually and independently because of the electrical diversity of the WPP. In practice, this is an advantage of a WPP compared to a conventional power plant. During a disturbance, the electrical characteristics at each terminal of the turbine is different from the other turbines, and only the most affected WTGs will be disconnected from the grid. For general faults (distance faults at the transmission point), only 5%-15% of the turbines are disconnected from the grid [3]. This is partially because WPPs are required to have zero voltage ride-through capability. Thus, the loss of generation is not as severe as in a power plant with large generators.

At the turbine level, the WTG generates at low voltage levels (480 V to 690 V). For the Type 1 and Type 2 WTGs, it is typically compensated by switched capacitor banks to generate at a unity power factor. Type 3 and Type 4 generators are operated to generate a constant voltage at a designated bus, or may be operated at constant power factor or constant reactive power. The generator is connected to a pad-mounted transformer to step up the voltage to 34.5 kV.

Collector System

The collector system consists of miles of line feeders connecting the high side of the pad-mounted transformer to the substation. Usually, wind turbines are divided into groups of turbines connected in a daisy chain fashion using underground cables. These groupings are then connected to the substation by either underground cables or overhead lines at 34.5 kV. Since it is not practical to model hundreds of turbines in a power flow calculation or in a dynamic simulation, it is common to find the equivalent of the turbines as either a single equivalent turbine representation or multiple turbine representation [4],[5].

Organization of the Paper

The organization of this paper is as follows; in section II, the SCC characteristics of different WTG types will be presented for a symmetrical fault. In section III, the characteristics of SCC for unsymmetrical faults will be discussed. Finally, in section V, the conclusion will summarize the paper's findings.

II. Short Circuit Behavior Under Symmetrical Faults

A utility-sized wind turbine is larger than non-grid wind turbine applications. In the early days, the turbines were sized from 10 kW to 100 kW. Nowadays, wind turbines are sized above 1000 kW (1 MW).

A. R-L Circuits

Short-circuit faults can occur in various locations of the power system in a number of different ways including line-to-ground and line-to-line faults. For simplicity purposes, we'll consider a symmetrical three-phase fault since it is the easiest to analyze. A simple equivalent diagram of a power system under such fault conditions is shown in Fig. 1a.

The fault in Fig. 1a is represented by a shorting switch. Immediately after the fault, the SCC contribution from the generator can be found using the following equation:

$$u_g = L\frac{di}{dt} + iR \qquad (1)$$

Where u_g is the instantaneous voltage on the generator terminals, and R and L are line resistance and inductance. Solving equation (1) for current

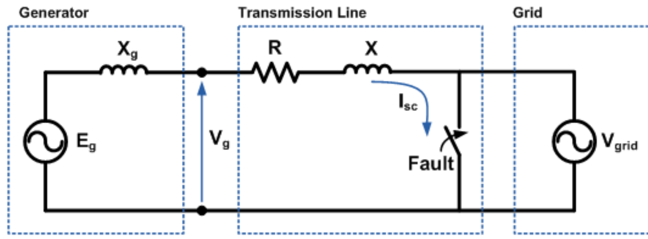

(a) Equivalent diagram of symmetrical fault

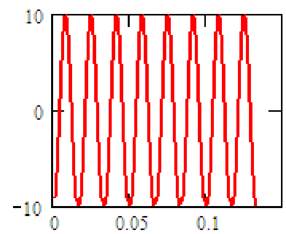

(b) AC component

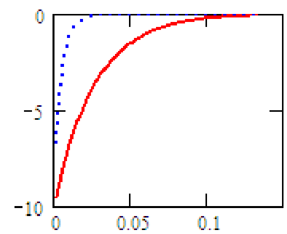

(c) DC component

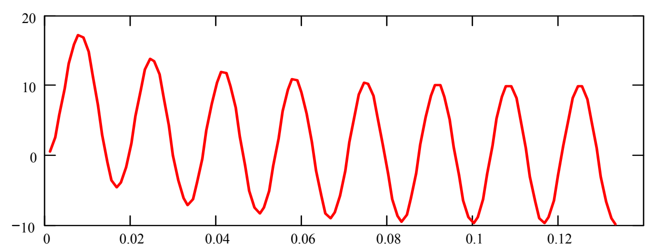

(d) Fault current

$$i = \frac{V_g}{Z}\sin\left(\omega t + \alpha - \operatorname{atan}\left(\frac{X}{R}\right)\right) - e^{-\frac{R}{L}t}\left[\frac{V_g}{Z}\sin\left(\alpha - \operatorname{atan}\left(\frac{X}{R}\right)\right)\right] \qquad (2)$$

Where V_g is peak generator voltage, $Z = \sqrt{R^2 + X^2}$ - line impedance, and α is the voltage phase. The solution (2) has two components; the first component is stationary and varies sinusoidally with time as shown in Figure 1b. It represents the steady SCC driven by the voltage source E_g. The second component decays exponentially (as shown in Figure 1c) with a time constant equal to $\frac{R}{L}$. It represents the DC component of the current and the natural response of the circuit without the excitation provided by E_g.

The steady-state symmetrical fault rms value of the SCC I_{sc} from the generator can be calculated from the first component of equation (2) and is shown in equation 3:

$$I_{sc} = \frac{V_g/\sqrt{2}}{\sqrt{R^2 + X^2}} \qquad (3)$$

Obviously, the steady-state fault current depends on the impedance of the line. The closer the fault occurrence location to generator terminals, the larger the SCC contributed to the fault.

The peak magnitude of the transient component in equation (2) depends on line impedance as well, but it also depends on impedance angle $\varphi = \text{atan}\left(\frac{X}{R}\right)$ at the point of the fault. The DC term does not exist if $\phi = 0$, and will have its maximum initial value of $\frac{V_g}{Z}$, where $\alpha - \varphi = \pm\frac{\pi}{2}$.

The worst case scenario for the SCC peak value (including the DC component) for the circuit presented in Figure 1a is shown in equation 3.

So, depending on the time when the fault occurs and the circuit characteristics, the transient current waveform will be different. This means that in three-phase systems, the phase transient currents will have different peaks due to a 120^0 shift in voltages.

In large power systems with many generators and transmission lines, the actual fault current at any location in the grid will be the sum of collective contributions from all generators, making the above described analysis extremely complicated. So, some sort of simplification is needed for the fault current calculation in such a case.

B. SCC from a Type 1 WTG

The first generation of utility-sized WTGs were a fixed-speed turbine with a squirrel-cage induction generator (SCIG) and is called a Type I generator in wind-related applications. The SCIG generates electricity when it is driven above synchronous speed. The difference between the synchronous speed and the operating speed of the induction generator is measured by its slip (in per unit or in percent). A negative slip indicates that the wind turbine operates in generating mode. Normal operating slips for an induction generator are between 0% and -1%. The simplified single-phase equivalent circuit of a squirrel-cage induction machine is shown in Fig. 2 [6].

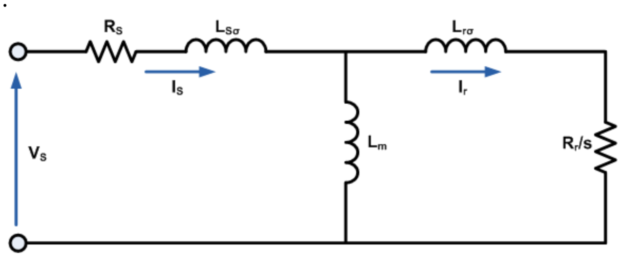

Fig. 2: Equivalent circuit of a Type 1 generator

The circuit in Fig. 2 is referred to the stator where R_S and R_r are stator and rotor resistances, $L_{s\sigma}$ and $L_{r\sigma}$ are stator and rotor leakage inductances, L_m is magnetizing reactance, and s is rotor slip. The example single-line connection diagram of a Type I generator is shown in Fig. 3. In the case of a voltage fault, the inertia of the wind rotor drives the generator after the voltage drops at the generator terminals. The rotor flux may not change instantaneously right after the voltage drop due to a fault. Therefore, voltage is produced at the generator terminals causing fault current flow into the fault until the rotor flux decays to zero. This process takes a few electrical cycles. The fault current produced by an induction generator must be considered when selecting the rating for circuit breakers and fuses. The fault current is limited by generator impedance (and can be calculated from parameters in Fig. 2) and impedance of the system from the short circuit to the generator terminals.

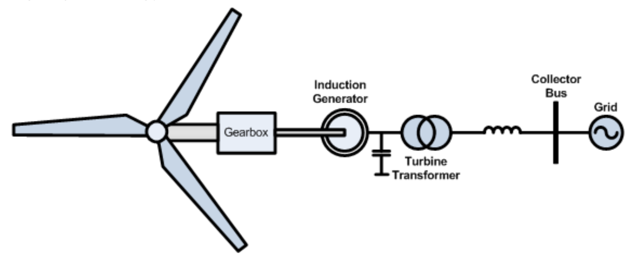

Fig. 3: Type 1 WTG

The initial value of fault current fed in by the induction generator is close to the locked rotor-inrush current. Assuming a three-phase symmetrical fault, an analytical solution can be found to estimate the current contribution of the generator. The SCC of an induction generator can be calculated as [7]:

$$i(t) = \frac{\sqrt{2}V_S}{Z_S'}\left[e^{-\frac{t}{T_S'}}\sin(\alpha) - (1-\sigma)e^{-\frac{t}{T_r'}}\sin(\omega t + \alpha)\right] \quad (4)$$

Where α is the voltage phase angle for a given phase, σ is the leakage factor, $Z_S' = X_S' = \omega L_S'$ is stator transient reac-

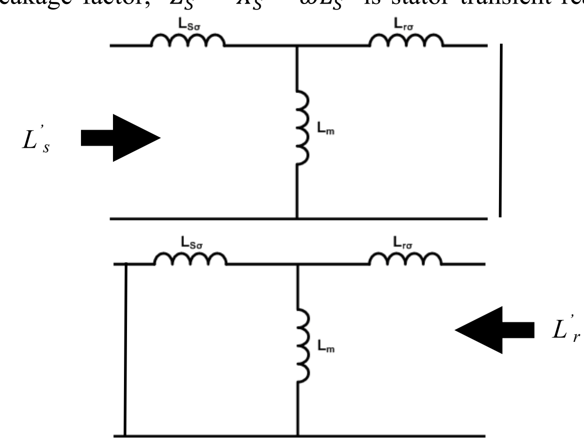

Fig. 4: Stator and rotor transient inductances.

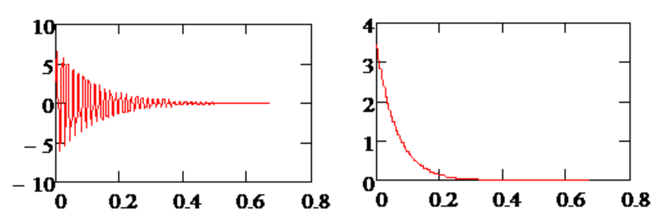

(a) AC component (b) DC component

Fig. 5: The two components of the SCC for a Type 1 WTG

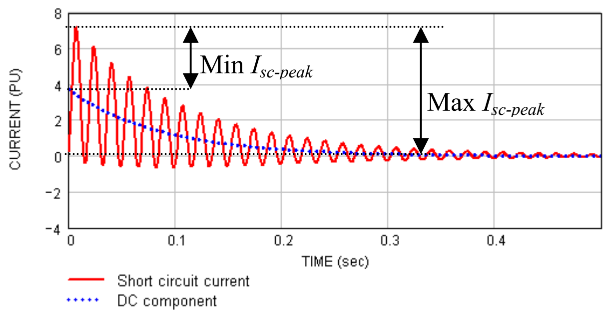

Fig. 6: SCC from a Type I WTG

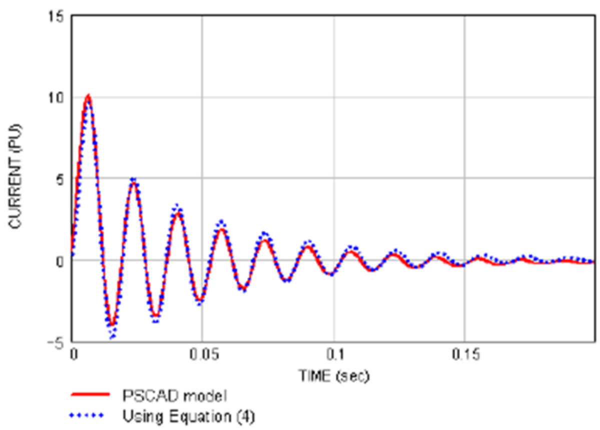

Fig. 7: SCC comparison between the output of the detailed model and the output of the simplified model simulated for a Type I WTG

tance, and $T_S^{'}$ and $T_r^{'}$ are stator and rotor time constants representing the damping of the DC component in stator and rotor windings. The transient stator and rotor inductances L_S' and L_r' can be determined from the circuits shown in Figure 4.

$$L_S' = L_{S\sigma} + \frac{L_{r\sigma}L_m}{L_{r\sigma}+L_m} \qquad L_r' = L_{r\sigma} + \frac{L_{S\sigma}L_m}{L_{S\sigma}+L_m} \quad (5)$$

$$T_S' = \frac{L_S'}{R_S}; \qquad T_r' = \frac{L_r'}{R_r} \quad (6)$$

$$\sigma = 1 - \frac{L_m^2}{L_S L_r} \quad (7)$$

$$L_S = L_{S\sigma} + L_m\,; \qquad L_r = L_{r\sigma} + L_m \quad (8)$$

Equation 4 is different from equation 2. The first distinction is that there is no voltage source driving the fault current as in equation 2. The fault current is driven by the decaying flux trapped in the rotor winding as represented by the right portion of the equation 4. The second distinction is the rotor time constant T_r' governs the dynamic of the decaying rotor flux (AC component of the SCC as shown in Fig. 5a) and the decaying DC component of the fault current (refer to Fig. 5b) is governed by the stator time constant T_S'. The larger the leakage inductances (σ), the smaller is the fault current amplitude. The third distinction is that the fault current dies out after the flux driving the fault current depleted to zero. Note, the DC and AC transient components of the SCC flowing out of the stator windings induce fault currents in the rotor winding and vice versa until the magnetic flux is depleted.

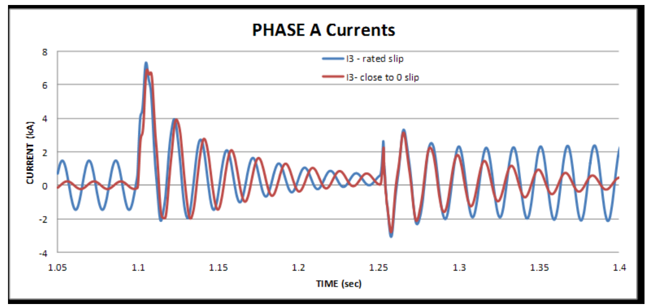

Figure 8: SCC comparison for two different slip.

The current calculated from equation (4) is shown in Fig. 6 using parameters for a typical 2-MW induction generator when and pre fault voltage 0.7 p.u. As can be seen from Fig. 6, the current reaches the maximum value at π (first half a period). Therefore, it may be a good approximation to calculate the maximum (peak) current by substituting $t = T/2$ into (4). The resulting equation for peak current will be:

$$i_{max} = \frac{\sqrt{2}V_S}{Z_S'}\left[e^{-\frac{T}{2T_S'}} + (1-\sigma)e^{-\frac{T}{2T_r'}}\right] \quad (9)$$

It was demonstrated experimentally in [8] that equation (9) gives satisfactory accuracy for peak current assessment. The resulting current is shown in Fig. 7. A detailed dynamic model of a Type 1 WTG is simulated in PSCAD™. A symmetrical three-phase fault is simulated and the resulting SCC is compared to the simulation result of the simplified representation as described in equation 4. It is shown in Fig. 7 that the two traces are very closely matched.

From equation 4, it is shown that the operating slip does not influence the short-circuit transient behavior. To check the influence of the slip, we performed symmetrical three-phase faults on a Type 1 WTG for two different slips using the detailed model. As shown in Fig. 8, the pre-fault current and the post-fault current for the two different operating slips are very distinct. Similarly, the frequencies of the SCC during the fault are not the same for two different operating slips. However, the peak values of the SCC of the induction generator operating at two different slips are very closely matched.

C. SCC from a Type 2 WTG

The variable slip generator is essentially a wound-rotor induction generator with a variable resistor connected in series to the rotor winding (Type 2 generator). This external resistor is controlled by a high-frequency switch. Below rated power, the resistor control is inactive, so the system operates as a conventional induction generator. Above rated power, the resistor control allows the slip to vary, so variable speed operation is possible for a speed range of about 10% [9]. If the blade pitch angle is kept constant at zero degrees, the rotor speed, and thus the slip, will vary with wind speed. However, operation at higher slips generate a lot of loss because of the rotor resistance. Thus, the heat loss can be excessive. On the other hand, if the blade pitch angle is controlled to keep the rotor speeds within a small deviation from the rated slip, the losses in rotor resistance can be minimized. An equivalent electrical diagram of a variable-slip induction generator is shown in Fig. 9, with a variable external resistor R_{ext}.

The connection diagram example for this type of generator is shown in Fig. 10. In case of three-phase symmetrical fault, the same equations as for a Type I generator are applied. The only difference will be for rotor time constant that needs to account for additional external resistance.

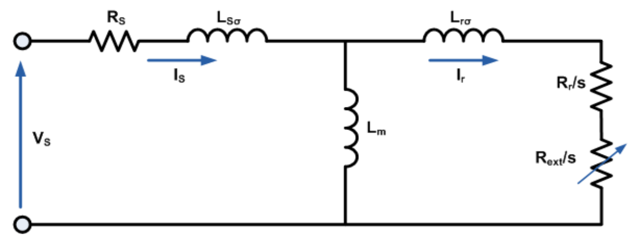

Fig. 9: Equivalent circuit for a Type 2 generator

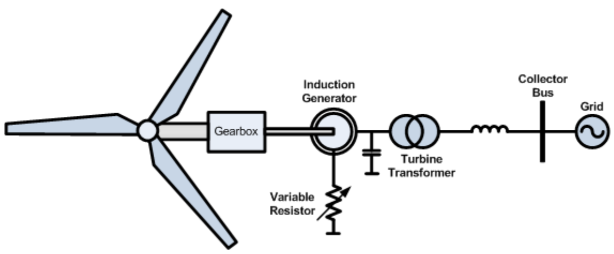

Fig. 10: Connection diagram for a Type 2 WTG

The modified rotor time constant can be calculated by adding the effect of the external resistor R_{ext} (refer to Table II, p. 7), where R_{ext} is the value of external resistance that happens to be in the circuit at the time of the fault. The effect of such additional resistance on SCC is shown in Fig. 11. So, adding the external resistors doubles the overall rotor resistance. The modified equation for SCC, maximum current, and the rotor transient time constant can then be derived using the values shown in Table I (see p. 7).

The maximum current occurs at ΔT, the time after a fault when current reaches its first peak. In this case, this additional resistance decreases the overall AC component in current, but does not much affect the first peak value of the current since the increase in resistance is relatively small. The same conclusion can be made by analyzing equations (4) and (9), where the additional external resistance has an effect on a second term that represents the AC component of the current. As shown in Table I and Table II, the impact of the external rotor resistance on the SCC is two-fold: it reduces the SCC magnitude, and it shortens the rotor time constant (decay time of the SCC).

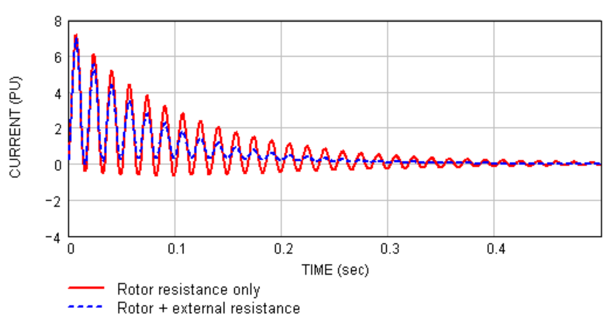

Fig. 11: Effect of external resistance for a Type 2 WTG

D. SCC from a Type 3 WTG

A Type 3 WTG is implemented by a doubly fed induction generator (DFIG). It is a variable-speed WTG where the rotor speed is allowed to vary within a slip range of $\pm$30%. Thus, the power converter can be sized to about 30% of rated power. The equivalent electrical diagram of a DFIG is shown in Fig. 12.

It is similar to one for a regular induction generator except for additional rotor voltage, representing voltage produced by a power converter. Under normal operation, this voltage is actually from a current-controlled power converter with the ability to control the real and reactive power output instantaneously and independently. The capability to control flux (flux-oriented controller – FOC) in induction machines has been used in the motor drive industry since the seventies.

The typical connection diagram for a DFIG (Type 3) WTG is shown in Fig. 12. In an ideal situation, the power converter connected to the rotor winding should be able to withstand the currents induced by the DC and AC components flowing in the stator winding. However, the components of the power converter (IGBT, diode, capacitor, etc.) are designed to handle only normal currents and normal DC bus voltage. A crowbar system is usually used for protecting the power electronics converter from overvoltage and thermal breakdown during short-circuit faults. A crowbar is usually implemented to allow the insertion of additional resistance into the rotor winding to divert the SCC in the rotor winding from damaging the power converter. Additional dynamic braking on the DC bus is also used to limit the DC bus voltage.

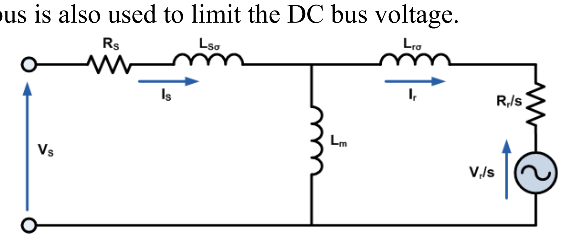

Fig. 12: Simplified equivalent circuit of a DFIG

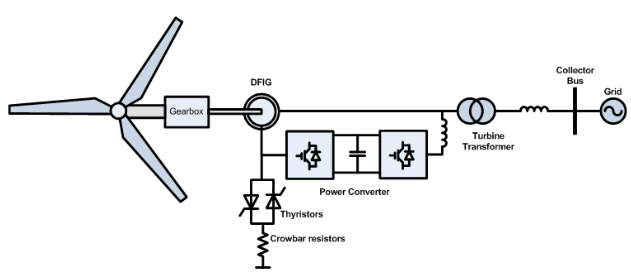

Fig. 13: Connection diagram for a Type 3 WTG

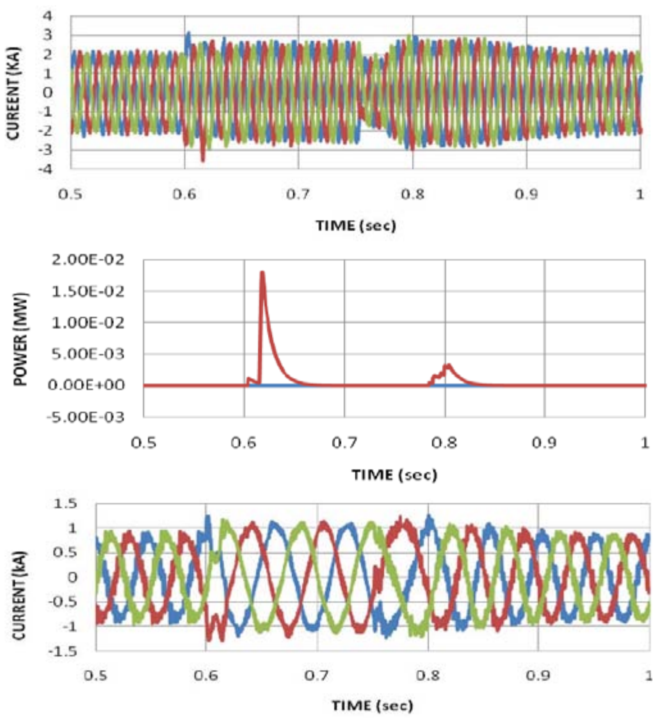

Fig. 14: The fault currents, the rotor currents, and the power consumed by the crowbar circuits in a Type 3 WTG.

During faults, the rotor windings are essentially short circuited by an equivalent adjustable crowbar resistance R_{CB}. The modified equation for SCC, maximum current, and the rotor transient time constant can then be derived using the values shown in Table I [7]. In a Type 3 WTG, however, the size of the crowbar is usually controlled as such that the actual fault current is more controllable than the simplified assumption. In Fig. 14, three-phase fault currents are shown to be well regulated by proper control of the crowbar resistance. In this case, the crowbar circuit installed on the rotor winding is controlled to maintain the DC bus voltage constant.

A dynamic braking resistor is also installed on the DC bus to help regulate the DC bus. Fig. 14 shows the size of the real power modulated in the crowbar during the faults. There are also dynamic braking resistors and a DC chopper installed on the DC bus to help regulate the DC bus voltage during transients. The corresponding rotor currents are also shown in Fig. 14. Because of differences in crowbar implementation from one turbine manufacturer to the other, a protection engineer should evaluate the recommended value provided by the manufacturers. However, if none is available, the values of minimum and maximum SCCs presented in Table I can be used.

E. Type 4 WTGs

An example of a Type 4 direct-drive WTG with permanent-magnet synchronous generator (PMSG) is shown in Fig. 15. This is a variable-speed WTG implemented with full power conversion. Recent advances and lower cost of power electronics make it feasible to build variable-speed wind turbines with power converters with the same rating as the turbines. The full power conversion allows separation between the WTG and the grid, thus, the mechanical dynamic can be buffered from entering the grid and the transient dynamic on the grid can be buffered from entering the wind turbine dynamic. Thus, while the grid is at 60 Hz, the stator winding of the generator may operate at variable frequencies. The temporary imbalance between aerodynamic power and generated power during a transient is handled by the pitch control, dynamic brake, and power converter control.

The SCC contribution for a three-phase fault is limited to its rated current or a little above its rated current. It is common to design a power converter for a Type 4 wind turbine with an overload capability of 10% above rated. Note that in any fault condition, the generator stays connected to the power converter and is buffered from the faulted lines on the grid. Thus, although there is a fault on the grid, the generator output current is controlled to stay within the current limit (e.g., 1.1 p.u.). However, keep in mind that with a fault on the grid, the output power delivered to the grid is less than rated power. Although the currents can be made to balance, due to reduced voltage and/or unbalanced voltage, only a reduced output power can be delivered. In Type 4 WTGs, the SCC is a controlled parameter. So, such WTGs can be represented as a constant 3-phase balanced current source in a short-circuit models. The priority of the real power versus reactive power during the fault depends on the prior setting of the controller. However, the current limit of the power converter must be followed to protect the power switches.

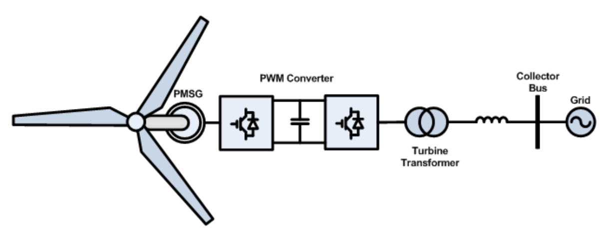

Fig. 15: PMSG direct-drive WTG diagram

F. SCC Comparison for Symmetrical Faults

The SCCs for different types of wind turbines are not the same. For each turbine types, the peak value of the magnitude of the SCC is affected by the transient reactance, the pre-fault voltage, the effective rotor resistances, and the instant the fault occurs.

For turbine Types 1 through Types 3, the SCC declines as the fault progresses and eventually ceases as the rotor flux is depleted. For Type 4 WTGs, the SCC can be maintained constant.

The SCC transient behavior is affected by the stator time constant and the rotor time constant for Type 1 through Type 3 WTGs. The Type 4 generators can generate constant current during the fault.

In Table I, the list parameters are shown. These parameters can be used to substitute the parameters from equation 4 and equation 6 for different types of WTGs. Table II lists the maximum and minimum possible values of the peak of SCC.

It is shown that the Type 1 WTG can produce the largest SCC. The instant of the fault has affects on the magnitude of the SCC. The maximum value is based on the peak of the AC component and the highest value of the DC component, and the minimum value is based on the peak value of the AC component only.

TABLE I.
MODIFIED VALUES FOR SCC CALCULATION FOR DIFFERENT TYPES OF WTGS

WTG	Type 1	Type 2	Type 3
Z'_s	$X'_S = \omega L'_S$	$\sqrt{X_S'^2 + R_{ext}^2}$	$\sqrt{X_S'^2 + R_{CB}^2}$
T'_r	$\frac{L'_r}{R_r}$	$\frac{L'_r}{R_r + R_{ext}}$	$\frac{L'_r}{R_r + R_{CB}}$

TABLE II.
MAXIMUM AND MINIMUM POSSIBLE VALUE OF THE SCC

WTG	Type 1	Type 2	Type 3	Type 4
Max I_{SC_PEAK}	$2\frac{\sqrt{2}V_s}{X'_s}$	$2\frac{\sqrt{2}V_s}{X'_s}$	$2\frac{\sqrt{2}V_s}{X'_s}$	1.1 I_{RATED}
Min I_{SC_PEAK}	$\frac{\sqrt{2}V_s}{X'_s}$	$\frac{\sqrt{2}V_s}{\sqrt{X_s'^2 + (9R'_r)^2}}$	1.1 I_{RATED}	0

For a Type 2 WTG, the maximum value is computed when R_{ext}= 0 Ω. The minimum value is computed when the slip reaches 10% above synchronous speed. And for a Type 3 WTG, the maximum value is computed when the crowbar shorts the rotor winding and the minimum value is computed when the power converter can follow the commanded current (i.e., in case the fault occurs far away from the point of interconnection, the remaining terminal voltage is relatively high enough to let the power converter operate normally and supply the commanded currents). Note, that for a symmetrical fault, the actual fault current for each phase is different from the other phases due to the fact that the time of the fault occurs at a different phase angle for different phases, thus affecting the DC offset. For a Type 4 WTG, the stator current can always be controlled because of the nature of power converter which is based on current controlled voltage source converter.

An example of SCC for Type 4 WTGs is given in the next section.

In this section, the SCC is analyzed at the terminals of the generator. In an actual WPP, the faults will likely occur at the transmission side. Thus, the impact of the cable capacitance, plant level reactive compensation, and wind plant transformer connections are not included. References [10-14] provide good sources of information for the WPP environment.

III. UNSYMMETRICAL FAULTS

The nature of the fault produces a different response for different wind turbine types. In this section, the observation of the short-circuit behavior for unsymmetrical faults on different types of WTGs will be presented. Note, that operating an induction generator under an unbalanced condition creates torque pulsation and unbalanced currents. If this condition persists for a long period of time, it may excite other parts of the wind turbine, and the unbalanced currents may create unequal heating in the three-phase windings, thus, shorten the life of the winding insulation.

Unlike in a symmetrical three-phase fault, the positive-sequence voltage source continues to drive the fault current until the fault or the generator removed from the circuit. The remaining un-faulted (normal) phases continue to maintain the air gap flux. The initial conditions of the fault currents are different for each phase. The three line currents usually show a different DC offset, which eventually settles out over time.

To explore the short-circuit behavior of unsymmetrical faults presented in this section, a detailed model of the system is developed in PSCAD™.

A. Single Line-to-Ground (SLG)Faults

The single line-to-ground fault is the most likely to occur in the power system. The magnetic flux in the air gap, although smaller than normal and unbalanced, is maintained by the remaining un-faulted lines. Thus, the short circuit in SLG faults will continue to flow until the circuit breaker removes the fault from the circuit.

Figure 16 shows the SCC of a Type 1 WTG for three lines-to-ground (3LG) and an SLG fault. In the symmetrical fault, the SCC dies out rather quickly, while in a SLG fault, the SCC is driven by the remaining two phases and it continues to flow until the short circuit is removed from the circuit. The peak current during a SLG fault is typically higher than for a 3LG fault (there is a quicker decay of current during symmetrical a 3LG fault due to magnetic field collapse). The differ-

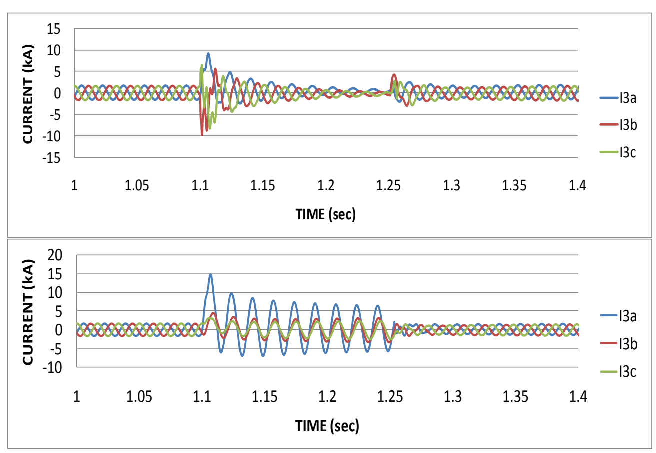

Fig. 16. Voltage and SCC for 3LG and SLG for a Type 1 WTG.

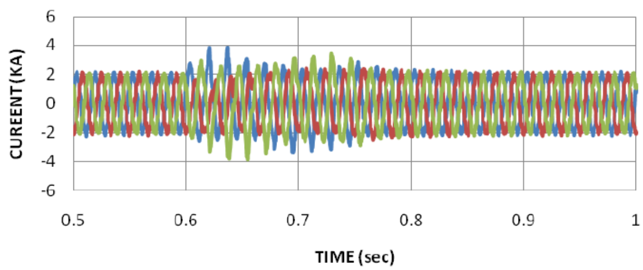

(a) Three phase currents

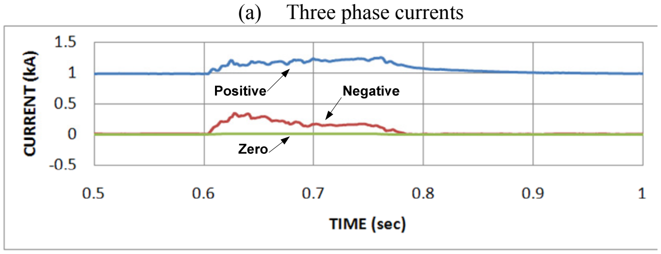

(b) Positive, negative and zero sequence currents

Fig. 17. SCC for SLG for a Type 3 WTG

ence in peak currents for both 3LG and SLG faults depends on generator parameters, fault location, etc. Note also that the presence of the positive sequence, the negative sequence, and zero sequence currents in the unsymmetrical faults influence the size of the SCC. No comparison has been made between dynamic simulation results and results obtained via symmetrical component calculations (this is planned for future work).

In Fig. 17, the SCC for a Type 3 WTG is shown both for the three-phase currents and the corresponding sequence components. The changes in positive sequence and the sudden appearance of the negative sequence are also shown. The absence of the zero sequence current is a consequence of transformer winding connections.

B. Line-to-Line (LL) and Line-to-Line-to-Ground (LLG) Faults

The line-to-line fault and the line-to-line-to-ground fault also maintained the air-gap flux during the fault. Output power of the generator will be limited and pulsating due to an unbalanced condition. The SCC will continue to flow until the circuit breaker removes the fault from the circuit.

As shown on Fig. 18 and Fig. 19, the type of fault affects the existence of the zero sequence component in the SCC of the WPP. Thus, the line currents in the three phases are distributed differently based on its positive sequence, negative sequence, and the zero sequence magnitudes and phase angles.

C. SCC for the Type 4 WTG under Different Faults

In Fig. 20, the fault currents for a Type 4 WTG are shown. Note, that the power converter buffers the generator from the grid. The SCC is basically controlled by the power converter. Hence, the line currents are symmetrical currents at different types of unsymmetrical faults. The post fault recovery may slightly differ for different faults.

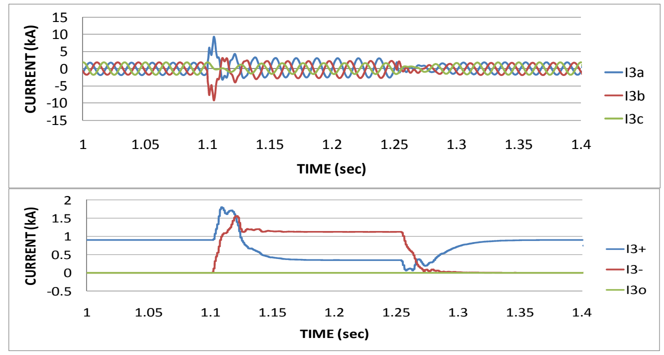

Fig. 18. The SCC for a LL fault of a Type 2 WTG.

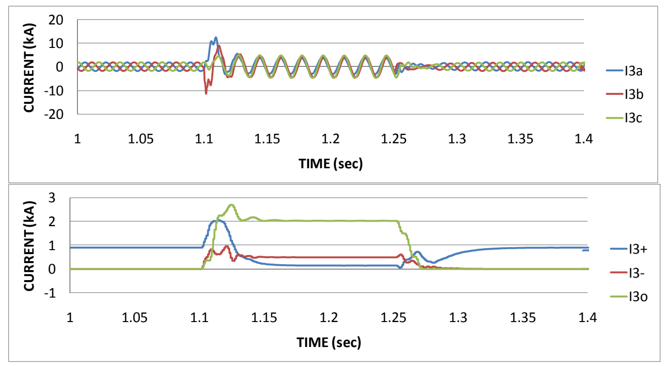

Fig. 19. The SCC for LLG fault of a Type 2 WTG.

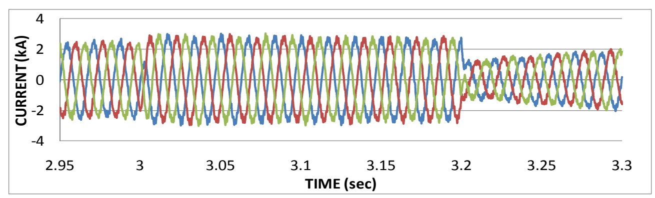

a) 3 LG

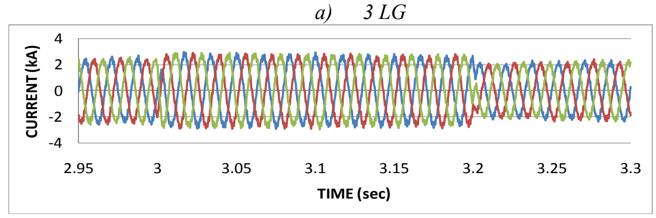

b) SLG

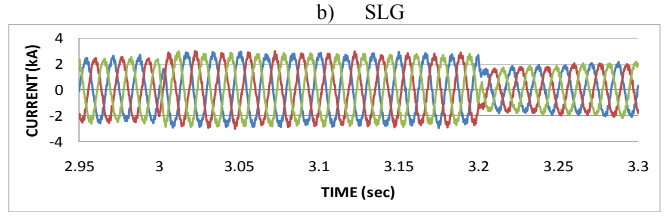

c) LLG

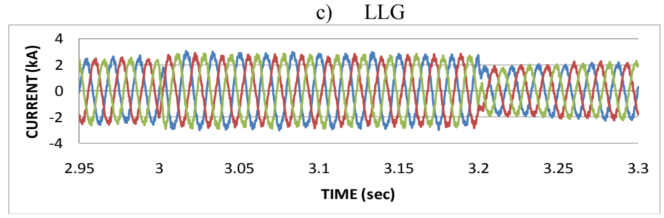

d) LL

Fig. 20. SCC for Type 4 WTG for different types of faults

IV. Conclusions

In this paper, the SCC contributions of different WTGs for faults at the terminal of the generator where simulated using simplified model to determine SCC characteristics for symmetrical faults. The simplified model represents the size and the time constants governing the SCC behavior. A table summarizing different fault impedance and transient rotor time constants is provided. Another table summarizing the range of SCCs for different types of WTGs is presented in Table II. For Type 1 and Type 2 WTGs, the maximum and the minimum values depend on timing of the fault, and the parameters and the operating condition of the induction generator. For Type 3 WTGs, the control and the operation of the crowbar and dynamic braking affects the characteristics of the SCC. For Type 4 WTGs, the SCC is controllable by the power converter.

To compute unsymmetrical faults, detailed models were used to demonstrate the behavior of SCCs of different WTGs. As expected, the SCC continues to flow until the fault is cleared from the circuit or the generator is disconnected from the grid. The terminal voltage and currents are sustained longer because the line voltages, except from the faulted phase, are able to sustain air gap flux. The nature of SCC is not only affected by the type of WTG, but also by the nature of the faults, and the winding connections of the generator and the transformers between the fault and the generator. Auxiliary components (reactive compensations), cable length and capacitance, the diversity of the WPP will contribute to the size and nature of the SCC, one way or another.

Each WPP is unique. Therefore, recommended practice from local reliability organizations, the manufacturers, transmission planners, wind plant developers, and the local utilities should be followed very closely.

V. Acknowledgment

This work is supported by the U.S. Department of Energy and California Energy Commission.

VI. References

[1] U.S. Department of Energy – Energy Efficiency and Renewable Energy, "20% Wind Energy by 2030 – Increasing Wind Energy's Contribution to U.S. Electricity Supply," May, 2008.
[2] J. Charles Smith, Michael R. Milligan, Edgar A. DeMeo and Brian Parsons, "Utility wind Integration and operating impact state of the art," *IEEE Trans. Power Systems*, vol. 22, pp. 900-908, Aug. 2007.
[3] E. Muljadi, Z. Mills, A. Ellis, R. Foster, " Fault Analysis at a Wind Power Plant for a One Year of Observation", presented at the IEEE Power Engineering Society, General Meeting, Pittsburgh, PA, July 20-24, 2008.
[4] E. Muljadi, S. Pasupulati, A. Ellis, D. Kosterev, "Method of Equivalencing for a Large Wind Power Plant with Multiple Turbine Representation", presented at the IEEE Power Engineering Society, General Meeting, Pittsburgh, PA, July 20-24, 2008.
[5] E. Muljadi, C. P. Butterfield, A. Ellis, J. Mechenbier, J. Hochheimer, R. Young, N. Miller, R. Delmerico, R. Zavadil, and J. C. Smith, "Equivalencing the collector system of a large wind power plant," in Proc. 2006 IEEE Power Engineering Society General Meeting.
[6] Nader Samaan, Robert Zavadil, J. Charles Smith and Jose Conto, "Modeling of Wind Power Plants for Short Circuit Analysis in the Transmission Network," in *Proc. of IEEE/PES Transmission and Distribution Conference*, Chicago, USA, April 2008.
[7] J. Moren, S.W.H. de Haan, "Short-Circuit Current of Wind Turbines with Doubly Fed Induction Generator," IEEE Transactions on Energy Conversion, Vol. 22, No. 1, March 2007.
[8] Sulawa, Zabara, et al. Short circuit current of induction generators. IEEE ISCAS 2007 proceedings.
[9] O. Anaya-Lara, N. Jenkins, et al. Wind energy generation: modeling and control. Wiley. ISBN 9780470714331
[10] IEEE PES Wind Plant Collector System Design Working Group,"Wind Power Plant Substation and Collector System Redundancy, Reliability and Economics," Proceedings of the 2009 IEEE Power and Energy Society General Meeting.
[11] IEEE PES Wind Plant Collector System Design Working Group, "Power Transformer Application for Wind Plant Substation," Proceedings of the 2009 IEEE Power and Energy Society General Meeting.
[12] IEEE PES Wind Plant Collector System Design Working Group, "Wind Power Plant Grounding, Overvoltage Protection, and Insulation Coordination," Proceedings of the 2009 IEEE Power and Energy Society General Meeting.
[13] WECC Modeling and Validation Work Group, "WECC Wind Power Plant Power Flow Modeling Guide Prepared." May 2008.
[14] Short-circuit currents in three-phase a.c. systems–Part 0: Calculation of currents, IEC Standard 60909-0, July 2001.

VII. Biographies

Eduard Muljadi (M'82-SM'94-F'10) received his Ph. D. (in Electrical Engineering) from the University of Wisconsin, Madison. From 1988 to 1992, he taught at California State University, Fresno, CA. In June 1992, he joined the National Renewable Energy Laboratory in Golden, Colorado. His current research interests are in the fields of electric machines, power electronics, and power systems in general with emphasis on renewable energy applications. He is member of Eta Kappa Nu, Sigma Xi and a Fellow of the IEEE. He is involved in the activities of the IEEE Industry Application Society (IAS), Power Electronics Society, and Power and Energy Society (PES).

He is currently a member of various committees of the IAS, and a member of the Working Group on Renewable Technologies and Dynamic Performance Wind Generation Task Force of the PES. He holds two patents in power conversion for renewable energy.

Vahan Gevorgian (M'97) graduated from the Yerevan Polytechnic Institute (Armenia) in 1986. During his studies, he concentrated on electrical machines. His thesis research dealt with doubly-fed induction generators for stand-alone power systems. He obtained his Ph.D. degree in electrical engineering. from the State Engineering University of Armenia in 1993. His dissertation was devoted to a modeling of electrical transients in large wind turbine generators.

Dr. Gevorgian is currently working at the National Wind Technology Center (NWTC) of National Renewable Energy Laboratory (NREL) in Golden, Colorado, USA, as a research engineer. His current interests include modeling and testing of various applications of small wind turbine based power systems.

REPORT DOCUMENTATION PAGE

Form Approved
OMB No. 0704-0188

1. REPORT DATE *(DD-MM-YYYY)* March 2011	**2. REPORT TYPE** Conference Paper	**3. DATES COVERED** *(From - To)*

4. TITLE AND SUBTITLE Short-Circuit Modeling of a Wind Power Plant: Preprint	**5a. CONTRACT NUMBER** DE-AC36-08GO28308
	5b. GRANT NUMBER
	5c. PROGRAM ELEMENT NUMBER
6. AUTHOR(S) E. Muljadi and V. Gevorgian	**5d. PROJECT NUMBER** NREL/CP-5500-50632
	5e. TASK NUMBER WE11.0825
	5f. WORK UNIT NUMBER
7. PERFORMING ORGANIZATION NAME(S) AND ADDRESS(ES) National Renewable Energy Laboratory 1617 Cole Blvd. Golden, CO 80401-3393	**8. PERFORMING ORGANIZATION REPORT NUMBER** NREL/CP-5500-50632
9. SPONSORING/MONITORING AGENCY NAME(S) AND ADDRESS(ES)	**10. SPONSOR/MONITOR'S ACRONYM(S)** NREL
	11. SPONSORING/MONITORING AGENCY REPORT NUMBER

12. DISTRIBUTION AVAILABILITY STATEMENT
National Technical Information Service
U.S. Department of Commerce
5285 Port Royal Road
Springfield, VA 22161

13. SUPPLEMENTARY NOTES

14. ABSTRACT *(Maximum 200 Words)*

This paper investigates the short-circuit behavior of a WPP for different types of wind turbines. The short-circuit behavior will be presented. Both the simplified models and detailed mod-els are used in the simulations and both symmetrical faults and unsymmetrical faults are discussed.

15. SUBJECT TERMS
Fault contribution; induction generator; electrical protection; short circuit; wind power plant; wind turbine

16. SECURITY CLASSIFICATION OF:			**17. LIMITATION OF ABSTRACT**	**18. NUMBER OF PAGES**	**19a. NAME OF RESPONSIBLE PERSON**
a. REPORT	**b. ABSTRACT**	**c. THIS PAGE**			
Unclassified	Unclassified	Unclassified	UL		**19b. TELEPHONE NUMBER** (*Include area code*)

Standard Form 298 (Rev. 8/98)
Prescribed by ANSI Std. Z39.18